Earthq Eng & Eng Vib (2008) 7:45-56 **DOI**: 10.1007/s11803-008-0823-x

Probabilistic fragility analysis: A tool for assessing design rules of RC buildings

Nikos D Lagaros†

Institute of Structural Analysis & Seismic Research,National Technical University of Athens,Greece

Abstract: In this work, fragility analysis is performed to assess two groups of reinforced concrete structures. The first group of structures is composed of buildings that implement three common design practices; namely, fully infilled, weak ground story and short columns. The three design practices are applied during the design process of a reinforced concrete building. The structures of the second group vary according to the value of the behavioral factors used to define the seismic forces as specified in design procedures. Most seismic design codes belong to the class of prescriptive procedures where if certain constraints are fulfilled, the structure is considered safe. Prescriptive design procedures express the ability of the structure to absorb energy through inelastic deformation using the behavior factor. The basic objective of this work is to assess both groups of structures with reference to the limit-state probability of exceedance. Thus, four limit state fragility curves are developed on the basis of nonlinear static analysis for both groups of structures. Moreover, the 95% confidence intervals of the fragility curves are also calculated, taking into account two types of random variables that influence structural capacity and seismic demand.

Keywords: probabilistic fragility analysis; design practice; behavior factor; Monte Carlo simulation method

1 Introduction

Over the last several decades, risk management of structural systems has gained the attention of various economic and technical professionals in modern society. The optimal allocation of public resources for a sustainable economy includes the need for rational tools to estimate the consequences of natural hazardous events on the built environment. The risk management process offers choices among different options that rely on technical and economic considerations. Risk assessment and decision analysis are the main steps in the risk management process. It is therefore essential to establish a reliable procedure to assess the seismic risk of structural systems. Seismic fragility analysis, which provides a measure of the safety margin of the structural system above specified hazard levels, is considered to be the central concept of risk assessment methods.

A number of methodologies for performing fragility analysis have been proposed in the past which have been used to assess the behavior of structural systems. Kennedy *et al*. (1980) presented a methodology for determining the probability of earthquake induced radioactive releases as a result of a core melt. Kircher *et al*. (1997) described building damage functions that were developed for the FEMA/NIBS (2003) earthquake loss estimation methodology. Shinozuka *et al*. (2000) presented a statistical analysis procedure for structural fragility curves. The significance of inherent randomness and modelling uncertainty in forecasting building performance was examined by Ellingwood (2001) through fragility assessment of a steel frame structure. The importance of fragility analysis in various stages of risk assessment, loss estimation, and decision making in consequence-based engineering to achieve the desirable long-term objectives of loss reduction and mitigation using the most efficient intervention measures was indicated in (Wen and Ellingwood, 2005). A procedure to account for the uncertainty of the characteristics of future ground motions during seismic response assessment was presented in Aslani and Miranda (2005). Fragility functions were developed in (Pagni and Lowes, 2006) to identify the method of repair required for older reinforced concrete beam-column joints damaged due to earthquake loading. A methodology for the risk assessment of reinforced concrete and unreinforced masonry structures was presented in Kappos *et al.*, (2006) and Jeong and Elnashai (2007) presented an approach where a set of fragility relationships with known reliability is derived based on the fundamental response quantities of stiffness, strength and ductility. A set of procedures

Correspondence to: Nikos D Lagaros, Institute of Structural Analysis & Seismic Research,National Technical University of Athens, 9, Iroon Polytechniou Str., Zografou Campus, 157 80 Athens, Greece
Tel: +30 210 772 2625; Fax: +30 210 772 1693
E-mail: nlagaros@central.ntua.gr
†Lecturer
Received January 19, 2008; **Accepted** January 23, 2008

for creating fragility functions from various kinds of data was introduced in (Porter *et al*., 2007). In the work by Shinozuka *et al*. (2003), bridge fragility curves are developed in order to determine the effect earthquakes have on the performance of transportation network systems.

The majority of reinforced concrete (RC) buildings are constructed with masonry infill walls. However, the combination of masonry infills with a framed structure is most often neglected during the design procedure, assuming that the contribution to structural performance is always positive. Such an assumption may lead to substantial inaccuracy in predicting the lateral stiffness, strength and ductility of the structure. In a number of studies (Lee and Woo, 2002; Negro and Verzeletti, 1996), the effect of weak ground stories on the seismic performance of RC frames was investigated. On the other hand, short columns at the ground story of a structure are prone to brittle shear failure, which may result in severe damage or even collapse due to poor ductility during earthquakes (Li, 2005; Guevara and Garcia, 2005).

All modern seismic design procedures are based on the principal that a structure will avoid collapse if it is designed to absorb and dissipate the kinetic energy that is imparted in it during seismic excitations. Most modern seismic codes express the ability of the structure to absorb energy through inelastic deformation using the behavior factor. The capacity of a structure to resist seismic actions in the nonlinear range generally permits their design for seismic loads smaller than those corresponding to a linear elastic response. The seismic loads are reduced using the behavior factor. The numerical confirmation of the behavior factor became a subject of research work during the past decade (Fajfar, 1998; Mazzolani and Piluso, 1996) in order to check the validity of design theory assumptions and to make structural performance more predictable from an engineering point of view.

The main objective of this study is to assess the way that weak ground story and short columns design practices are implemented, and to examine the influence of the behavioral factor used to define the seismic design forces on the final design. Therefore, two groups of structures are compared with reference to the limit-state fragilities developed in four drift-based limit states. Moreover, statistical analysis is performed on the fragility curves defining the 95% confidence intervals considering randomness in both structural capacity and seismic demand.

2 Fragility analysis

Earthquake risk assessment of building structures requires calculation of limit-state probabilities for a series of limit-states of monotonically increasing severity. The objective is to obtain the limit-state probabilities of exceedance that will serve as a hazard curve for structural damage. The mean annual frequency of the maximum interstory drift $\theta_{\max}$ exceeding the value y is obtained as:

$$P(\theta_{\max} \geq y) = \int P\left(\theta_{\max} \geq y / IM = x\right) \left|\mathrm{d}\lambda_{IM}(x)\right| \tag{1}$$

where $P\left(\theta_{\max} \geq y / IM = x\right)$ is the probability that $\theta_{\max}$, exceeds the value y given that IM equals x and $\lambda_{IM}(x)$ is the mean annual frequency of the chosen intensity measure exceeding x, or in other words $\lambda_{IM}(x)$ is the hazard curve and $\mathrm{d}\lambda_{IM}(x)$ is its slope. The absolute value is used because the slope has a negative value.

Building fragility curves are lognormal functions that describe the probability of reaching or exceeding a specific limit state. The conditional probability of being, or exceeding, a particular damage state y given peak ground acceleration (PGA), a_{PG} (or other seismic demand parameter) is defined by:

$$P\left(\theta_{\max} \geq y \mid a_{\mathrm{PG}}\right) = \Phi\left[\frac{1}{\beta_y} \ln\left(\frac{a_{\mathrm{PG}}}{\bar{a}_{\mathrm{PG},y}}\right)\right] \tag{2}$$

where $\bar{a}_{\mathrm{PG},y}$ is the median value of peak ground acceleration where the building reaches the threshold of damage state y, β_y is the standard deviation of the natural logarithm of peak ground acceleration for the damage state y, and Φ is the standard normal cumulative distribution function.

3 Seismic design procedures

The majority of seismic design codes are prescriptive in nature, and include procedures for site selection and development of conceptual, preliminary and final design stages. According to a prescriptive design code, the strength of the structure is evaluated at one limit state between life-safety and near collapse using a response spectrum corresponding to a design earthquake (EAK 2000; Eurocode 8, 2003). In addition, the serviceability limit state is checked to ensure that the structure will not deflect or vibrate excessively during its lifetime. The main principle of new provisions, such as EAK 2000 and Eurocode 8 (2003), is to design structural systems based on energy dissipation and on ductility to control the inelastic seismic response. Designing a multistory RC building for energy dissipation comprises the following features: (i) fulfillment of the strong column/weak beam rule; (ii) member verification in terms of forces and resistances for the ultimate strength limit state under a design earthquake (with a return period of 475 years, and a probability of exceedance of 10% in 50 years), with the elastic spectrum reduced by the behavior factor; (iii) damage limitation for the serviceability limit state; and (iv) capacity design of beams and columns against shear failure.

According to the Greek national design codes and

Eurocodes, a number of checks must be considered to ensure that the structure will meet the design requirements. All EKOS 2000 or Eurocode 2 (2002) checks must be satisfied for gravity loads using the following load combination

$$S_{\mathrm{d}} = 1.35\sum_j G_{kj} "+" 1.50\sum_i Q_{ki} \tag{3}$$

where "+" implies "to be combined with", the summation symbol "Σ" implies "the combined effect of", G_{kj} denotes the characteristic value "k" of the permanent action j, and Q_{ki} refers to the characteristic value "k" of the variable action i. If the above constraints are satisfied, multi-modal response spectrum analysis is performed, according to EAK 2000 and Eurocode 8 (2003), and earthquake loading is considered using the following load combination

$$S_{\mathrm{d}} = \sum_j G_{kj} "+" E_{\mathrm{d}} "+" \sum_i \psi_{2i} Q_{ki} \tag{4}$$

where E_{d} is the design value of the seismic action for the two components (longitudinal and transverse), respectively, and ψ_{2i} is the combination coefficient for quasi-permanent action i, here taken to be equal to 0.30.

4 Design practices

The behavior of a building during an earthquake depends on its overall shape, size and geometry. A wide range of structural damage observed during past earthquakes around the world has been very educational in identifying construction features related to the shape, size and geometry of a structure that must be avoided. Buildings that have fewer columns or are fully infilled in some stories, or have partially infilled stories, tend to be more vulnerable to earthquake loading. A large number of multi-story RC buildings collapsed in past earthquakes, due to construction features such as weak stories, short columns, strong beams-weak columns, large and heavy overhangs and others (Dolsěk and Fajfar, 2001; Ghobarah *et al*., 2006; Chao *et al*., 2006; Mitchell *et al*., 1996).

4.1 Weak ground story

RC building structures have become very popular during the last decades in urban Greece. Many such buildings constructed in recent times have a special construction feature; the ground story is left open for the purpose of parking. Such buildings are also called weak ground story buildings, while the weak story is also called a soft story or *pilotis*. Weak ground story buildings have shown poor performance during past earthquakes around the world (Dolsěk and Fajfar, 2001; Ghobarah *et al*., 2006); and a significant number of them have collapsed. The fully infilled upper stories are much stiffer than the open ground story. Thus, the upper stories deform almost together, and the maximum interstory drift occurs in the weak ground story. Consequently, the columns in the open ground story are severely stressed. If the columns do not have the required strength to resist or do not have adequate ductility, they may be severely damaged, which may then lead to the collapse of the building.

4.2 Short columns

In past earthquakes, RC buildings with short columns suffered from damage (Chao *et al*., 2006; Mitchell *et al*., 1996), due to the concentration of large shear forces. The short columns are stiffer compared to regular size columns and attract larger earthquake forces. If a short column is not adequately designed for such a large force, it can suffer significant damage during an earthquake. Short columns are characterized by a small value of the shear span ration α:

$$\alpha = \frac{M_{\mathrm{sd}}}{V_{\mathrm{sd}} h} \le 2.5 \tag{5}$$

where M_{sd} and V_{sd} are the maximum moment and shear force values obtained from the combination of Eq. (4) while h is the column depth. Generally speaking, the failure modes of short columns can be classified into two cases: (i) shear failure, which occurs when $\alpha \le 1.50$; and (ii) sliding failure, which occurs when $1.5 - 2.0 \le \alpha \le 2.5$.

5 Confidence intervals

In this work, in order to define the 95% confidence intervals for each fragility curve developed, the procedure suggested by Shinozuka *et al*. (2000) was followed. In particular, the Monte Carlo Simulation (MCS) method was used to generate 10,000 simulations on the basis of nonlinear static analysis in both the examples. Two sources of randomness were considered: ground motion excitation that influences the level of seismic demand, and material properties that affect the structural capacity. The modulus of elasticity of concrete, steel reinforcement and masonry infill along with the compressive strength, yield strain and ultimate strain for both confined and unconfined concrete were taken as random variables influencing the structural capacity. More detailed description of the random variables affecting the structural capacity for both test examples are given in the numerical study section.

The randomness on the seismic excitation is considered through the response spectra. For this purpose, a set of natural records that consist of both longitudinal and transversal components of the records, are used. The records were selected from the database of Somerville and Collins (Somerville and Collins, 2002) corresponding to the hazard level with 10 percent probability of being exceeded in 50 years (Table 1).

The records are scaled to the PGA value obtained from hazard curves originally derived for Greece by Papazachos *et al*. (1993). Moreover, based on the assumption that seismic data follow the lognormal distribution (Chintanapakdee and Chopra, 2003), the median spectrum $\hat{x}$ and the standard deviation δ can be calculated using the following expressions:

$$\hat{x} = \exp\left[\frac{\sum_{i=1}^{n}\ln(R_{\mathrm{d},i}(T))}{n}\right] \tag{6}$$

$$\delta = \left[\frac{\sum_{i=1}^{n}\left(\ln(R_{\mathrm{d},i}(T)) - \ln(\hat{x})\right)^2}{n-1}\right]^{1/2} \tag{7}$$

where $R_{\mathrm{d},i}(T)$ is the response spectrum value for period equal to T of the i-th record (i=1,…,n) and the number of records used and varies for different hazard levels. Therefore, n = 19 for the 10% in 50 years case. Both components of the median spectra are shown in Fig. 1.

Table 1 Natural records

Earthquake	Station	Distance	Site
Tabas (TB) 16 September 1978	Dayhook	14	rock
	Tabas	1.1	rock
Cape Mendocino (CM) 25 April 1992	Cape Mendocino	6.9	rock
	Petrolia	8.1	soil
Chi-Chi (CC), Taiwan 20 September 1999	TCU052	1.4	soil
	TCU065	5.0	soil
	TCU067	2.4	soil
	TCU068	0.2	soil
	TCU071	2.9	soil
	TCU072	5.9	soil
	TCU074	12.2	soil
	TCU075	5.6	soil
	TCU076	5.1	soil
	TCU078	6.9	soil
	TCU079	9.3	soil
	TCU089	7.0	rock
	TCU101	4.9	soil
	TCU102	3.8	soil
	TCU129	3.9	soil

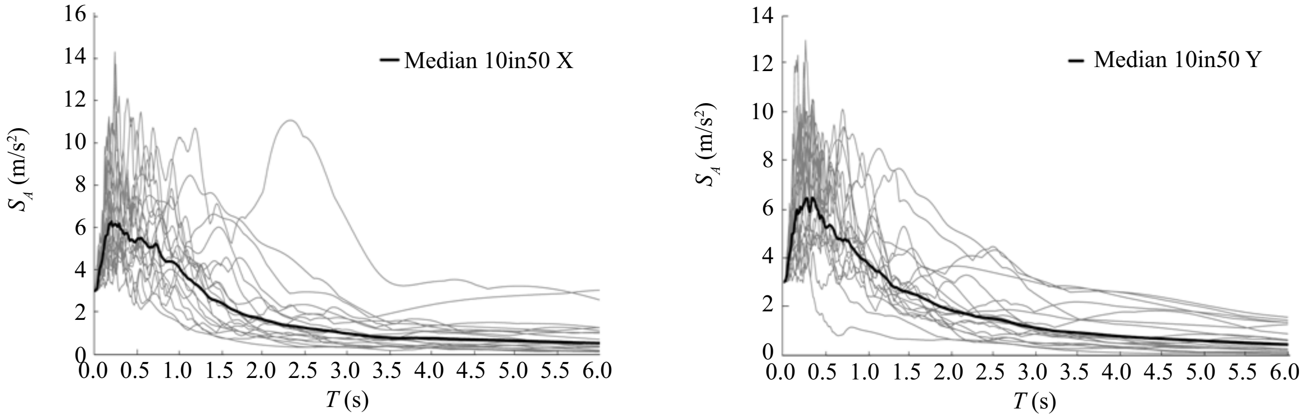

(a) Longitudinal(x) (b) Transverse(y)

Fig. 1 Natural records response spectra and their median

6 Numerical study

Two test examples have been considered to perform the fragility analysis. For both test examples, the lateral design forces were derived from the design response spectrum, i.e., 5%-damped elastic spectrum divided by the behavior factor at the fundamental period of the building. Concrete of class C16/20 (nominal cylindrical strength of 16MPa) and class S500 steel (nominal yield stress of 500MPa) are assumed. The base shear is obtained from the response spectrum for soil type A (stiff soil θ = 1, with characteristic periods T_1 = 0.10 s and T_2 = 0.40 s) in the first test example and soil type B (stiff soil θ = 1.0, with characteristic periods T_1 = 0.15 s and T_2 = 0.60 s) for the second one. The PGA value is equal to 0.31 g, corresponding to zone III for the 10/50 hazard level. Greece is divided into three zones of equal seismic hazard. Papazachos *et al*. (1993) have presented a semi-probabilistic approach to the seismic hazard assessment of Greece resulting in hazard curves for all zones. The city of Athens, which is where the two test examples will be built, belongs to zone III. Moreover, the importance factor γ_I was taken to be equal to 1.0, while the damping correction factor is equal to 1.0, since a damping ratio of 5% was considered (as suggested by EAK 2000 for RC structures).

For both test examples, the slab thickness is equal to 15 cm and is considered to contribute to the moment of inertia of the beams with an effective flange width. In addition to the self weight of the beams and the slab, a distributed dead load of 2 kN/m^2 due to floor finishing and partitions is considered, while live load with a nominal value of 1.5 kN/m^2 is also applied. In the combination of gravity loads ("persistent design situation"), nominal dead and live loads are multiplied with load factors of 1.35 and 1.5, respectively. Following EAK 2000, in the seismic design combination, dead loads are considered with their nominal value while live loads are considered to be 30% of the nominal values. For all test cases, a centerline model was formed based on the OpenSEES (McKenna and Fenves, 2001) simulation platform. The members are modelled using the force-based fiber beam-column element while the same material properties are used for all the members of the test cases examined. Soil-structure interaction was not considered and the base of the columns at the ground floor is assumed to be fixed.

6.1 Test example 1

The first test example is the 3D RC building shown in Fig. 2, with four stories analyzed first by Lagaros (2007). The lateral design forces were derived from the design response spectrum described above while a behavior factor q equal to 3.5 is considered, as suggested by EAK 2000 for RC structures. The cross section for all columns is 45cm×45cm and 30cm×60cm for all beams. The infill walls consists of 30cm×20cm×15cm horizontally perforated bricks with a compressive strength equal to 3.0 MPa and a modulus of elasticity equal to 2250 MPa. ELSA laboratory (Negro and Verzeletti, 1996) models, similar to the ones examined in this study, have also been tested.

The model employed in this study for simulating the masonry infill panels is based on the one developed by Perera *et al*. (2004). According to this model, the contribution of the masonry infill panel to the response of the infilled frame is modeled by a system of two diagonal masonry compression struts. The two struts are considered ineffective in tension since the tensile strength of masonry is negligible. The combination of both diagonal struts provides the lateral load resisting mechanism for the opposite lateral directions of loading. Each strut element is modeled as a simple longitudinal inelastic spring whose behavior is described in terms of the axial force-axial deformation relationship of the strut

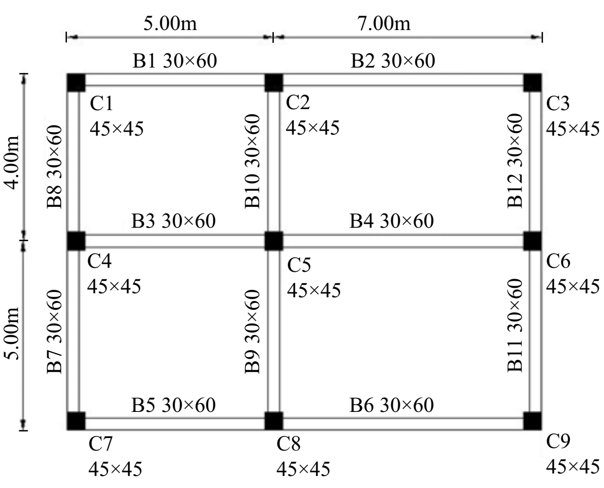

(a) Layout

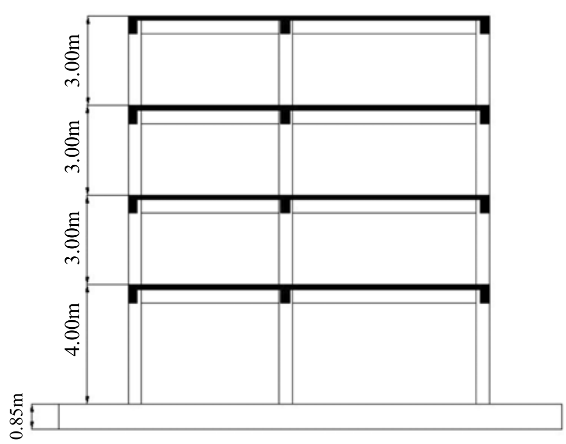

(b) Front view

Fig. 2 Test example 1 - Geometry of the three storey 3D building

using the notion and principles of continuum damage mechanics. In the work by Perera *et al*. (2004), the following relationship was obtained:

$$N = K_0(1-d)\delta^e = K_0(1-d)(\delta - \delta^p) \tag{8}$$

where N is the axial force of the strut, δ, δ^e and δ^p are the total, elastic and plastic shortenings of the strut, respectively. K_0 is the initial stiffness before cracking and d is the internal damage variable representing the degradation of the infill. More details about the damage model of the masonry infill used in this work can be found in Perera *et al*. (2004).

6.1.1 Description of the test cases

For this test example, three different cases were examined: (i) fully infilled model that corresponds to the design where all circumferential frames in all stories are considered fully infilled (see model in Fig. 3(a)); (ii) weak ground story model, where no masonry infill are present in the ground story (see model in Fig. 3(b)); and (iii) short columns model, where transverse frames C3-B12-C6-B11-C9 and C1-B8-C4-B7-C7 are fully infilled (see model in Fig. 3(a) and longitudinal frames C1-B1-C2-B2-C3 and C7-B5-C8-B6-C9 are partially infilled in the ground level (see model in Fig. 3(c)). All models were designed to meet the EKOS 2000 and EAK 2000 requirements, implementing all the provisions suggested by the codes in order to alleviate the effect of the design practices on the structural performance. The weight of the steel reinforcement and the concrete volume required for the three models are given in Table 2. As seen, the concrete volume is the same since the cross section for all columns and beams is equal to 45cm×45 cm and 30cm×60cm, respectively, for all three designs. The difference in the reinforcement of the columns and the beams is due to the implementation of the code provisions for the various design practices. As seen from Table 2, the fully infilled design requires less reinforcement than the others, while the weak ground story design requires the most reinforcement.

6.1.2 Fragility analysis-confidence intervals

Figures 4(a) to 4(d) depict the limit state fragility curves for RC buildings for the Slight, Moderate, Extensive and Complete structural damage states. The limit states are defined with respect to the drift limits given by Ghobarah (2004). For the fully infilled case, the drift limits defining the damage states are equal to 0.1%, 0.4%, 0.7% and 0.8% for Slight, Moderate, Extensive and Complete structural damage states, respectively. For the bare frame, the drift limits become 0.2%, 1.0%, 1.8% and 3.0% for the four damage states, respectively. In Figs. 4(a) to 4(d), the PGA value of the design earthquake in EKOS 2000 is denoted with a bold vertical line and the corresponding limit-state probabilities of exceedance are given in Table 3. Note that although the probability of exceedance for the fully infilled design for the Slight damage state is almost the same with that of the weak ground story and short columns designs (87% versus 100%), the probability of exceedance for the Moderate damage state of the fully infilled design is one order of magnitude less than the corresponding probability of the other two designs (4.5% versus 97.0%), while for the Complete damage state, the probability of exceedance for the fully infilled design is three orders of magnitude less than the corresponding probability of the other two

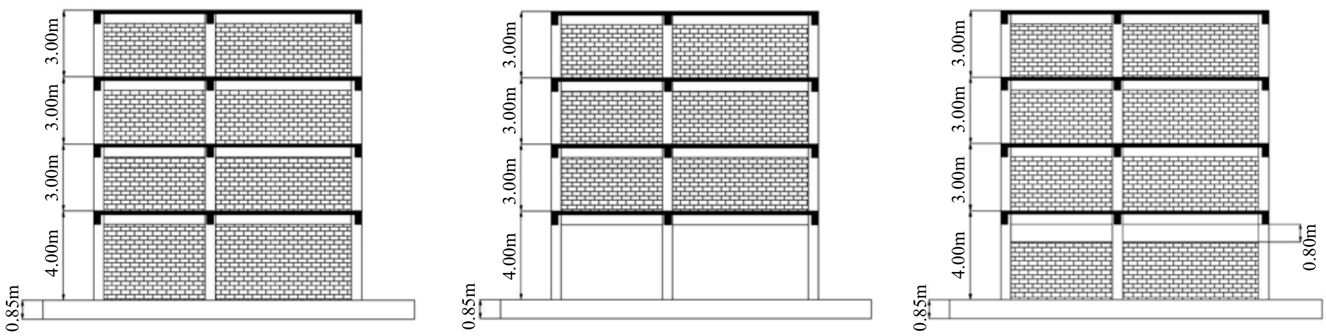

Fig. 3 Test example 1 - The models for the C7-B5-C8-B6-C9 frame

Table 2 Test example 1 - Comparison of steel and concrete quantities

Model	Columns		Beams	
	Steel (kg)	Concrete (m^3)	Steel (kg)	Concrete (m^3)
Fully infilled	5868	23.7	5495	39.5
Weak ground storey	6516	23.7	5794	39.5
Short columns	6210	23.7	5495	39.5

designs (0.02% versus 42.0% and 13.0%).

In order to define the 95% confidence intervals for all fragility curves, two sources of randomness have been taken into account: (i) those affecting the structural capacity (f_c: compressive strength, $\varepsilon_{c,y}$: yield compressive strain, $\varepsilon_{c,u}$: ultimate compressive strain, E_c: concrete modulus of elasticity, f_y: steel yield stress, E_s: steel modulus of elasticity, f_{inf}: perforated brick compressive strength, E_{inf}: perforated brick modulus of elasticity); and (ii) those affecting the seismic demand. Details on

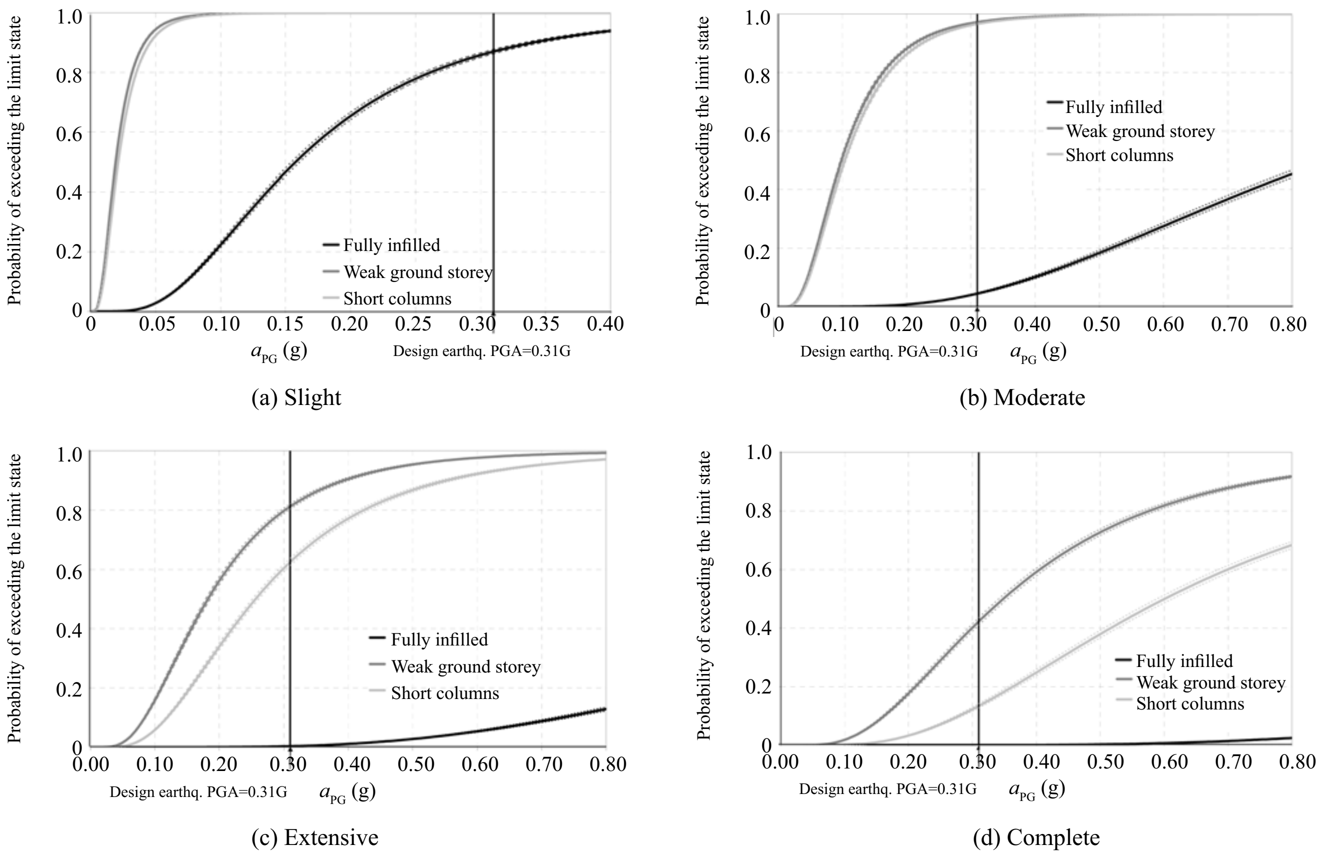

Fig. 4 Test example 1 - Fragility curves for the four limit states and their confidence intervales

Table 3 Test example 1 – Limit-state probability of exceedance

%

Limit state		Fully infilled	Weak ground storey	Short columns
Slight	Mean	87.03	100.00	100.00
	+	87.73	100.00	100.00
	-	86.32	100.00	100.00
Moderate	Mean	4.46	97.22	96.60
	+	4.78	97.42	96.84
	-	4.16	97.01	96.34
Extensive	Mean	0.33	81.21	62.47
	+	0.37	82.11	63.70
	-	0.30	80.30	61.26
Complete	Mean	0.02	42.28	13.44
	+	0.02	43.58	14.17
	-	0.02	41.01	12.75

Table 4 Test example 1 - Characteristics of the random variables

Parameter	Distribution	Mean value	COV	Correlation
Confined concrete				
f_c (MPa)	Normal	16.0	0.15	0.3
$\varepsilon_{c,y}$	Normal	0.002	0.15	0.3
$\varepsilon_{c,u}$	Normal	0.0035	0.15	0.3
Unconfined concrete				
f_c (MPa)	Normal	12.8	0.15	0.3
$\varepsilon_{c,y}$	Normal	0.002	0.15	0.3
$\varepsilon_{c,u}$	Normal	0.0035	0.15	0.3
E_c (GPa)	Normal	28.0	0.15	0.3
Steel				
f_y (MPa)	Normal	500.0	0.05	0.5
E_s (GPa)	Normal	200.0	0.05	0.5
Masonry infill				
F_{inf} (MPa)	Normal	3.0	0.15	0.3
E_{inf} (GPa)	Normal	2.25	0.15	0.3
Seismic action				
Seismic Load	Lognormal	$\hat{x}$ (Eq. (6))	δ (Eq. (7))	0.0

the two sources of randomness are shown in Table 4. Confidence intervals for the four sets of fragility curves are also depicted in Figs. 4(a) to 4(d), while the 95% confidence intervals of the probability of exceedance of the four limit states for the design earthquake are shown in Table 3.

6.2 Test example 2

The three story bare 3D RC building (see Fig. 5) first analyzed by Lagaros *et al*. (2006) is used as the second test example of this work. The 3D RC building was designed to meet the EKOS 2000 and EAK 2000 requirements for different values of the behavior factor q ranging from 1.0 to 6.0 with a step size equal to 1.0, while all six cases were designed as bare frames.

6.2.1 Description of the test cases

The parametric study resulted in six different designs, depending on the value of the behavioral factor q. The design process for the Greek design code started with the same initial design having the same minimum dimensions for the beams and the columns. The minimum dimensions considered were as follows: columns 25cm×25cm and beams 25cm×30cm. The dimensions of the columns and the beams were increased until the requirements and provisions of the EAK 2000 were fulfilled for the current value of the behavior factor q. Beams and columns that did not meet the constraints imposed by EAK and EKOS design codes were increased in size according to the following procedure: (i) *columns*: increase the size of the smallest dimension by 5 cm and if column constraints are not yet satisfied, increase the size of the second dimension by 5 cm; this rule is processed until all the constraints are satisfied; (ii) *beams*: increase the size of the height of the beam by 5 cm and if constraints are not yet satisfied, increase the width of the web by 5 cm (the with width of the web is restricted not to exceed 35 cm) until all the constraints are satisfied, similar to the method used for the columns. The weight of the steel and the concrete quantities required for the six designs using the Greek national design codes are given in Table 5.

6.2.2 Fragility analysis-confidence intervals

Figures 6(a) to 6(d) depict the limit state fragility curves for RC buildings for the Slight, Moderate, Extensive and Complete structural damage states. As in the previous test example, the limit states are defined with respect to the drift limits given in (Ghobarah, 2004) for the bare frame. In Figs. 6(a) to 6(d), the PGA value for the design earthquake for EKOS 2000 is denoted with a bold vertical line and the corresponding probabilities of exceedance of the four damage states are given in Table 6. In order to evaluate the performance of the different designs achieved, three characteristic designs were selected. These designs correspond to the two extreme designs with respect to the value of the behavioral factor q. The first extreme design, denoted as $D_{q=1}$, is the one achieved for q=1 (permitting linear behavior only) and the second extreme design is denoted as $D_{q=6}$, corresponding to the largest value of the behavior factor examined in this study. The third design, denoted as $D_{q=3}$, corresponds to the design obtained for q=3.0.

The probability of exceedance of the $D_{q=1}$ design for the Slight damage state is almost the same as the corresponding $D_{q=3}$ and $D_{q=6}$ designs (66% versus 100%). The probability of exceedance of the Moderate damage

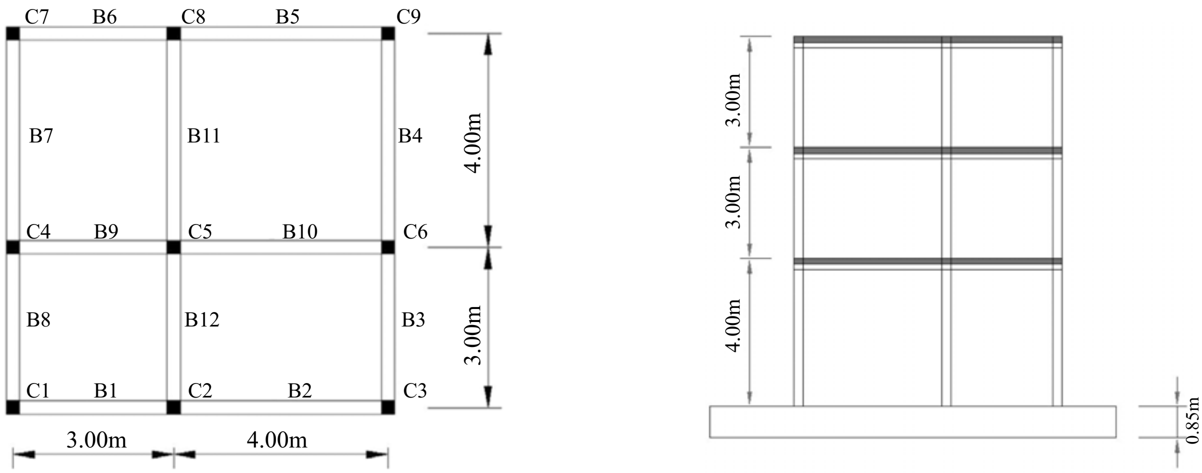

(a) Layout (b) Front view

Fig. 5 Geometry of the three storey 3D building

Table 5 Test example 2 - Comparison of steel and concrete quantities

Design procedure	Columns		Beams	
	Steel (kg)	Concrete (m^3)	Steel (kg)	Concrete (m^3)
$D_{q=1}$	12700	32	6940	27
$D_{q=2}$	7720	21	4180	17
$D_{q=3}$	5730	15	3170	13
$D_{q=4}$	4600	14	2490	11
$D_{q=5}$	4010	12	2140	11
$D_{q=6}$	3750	11	1940	10

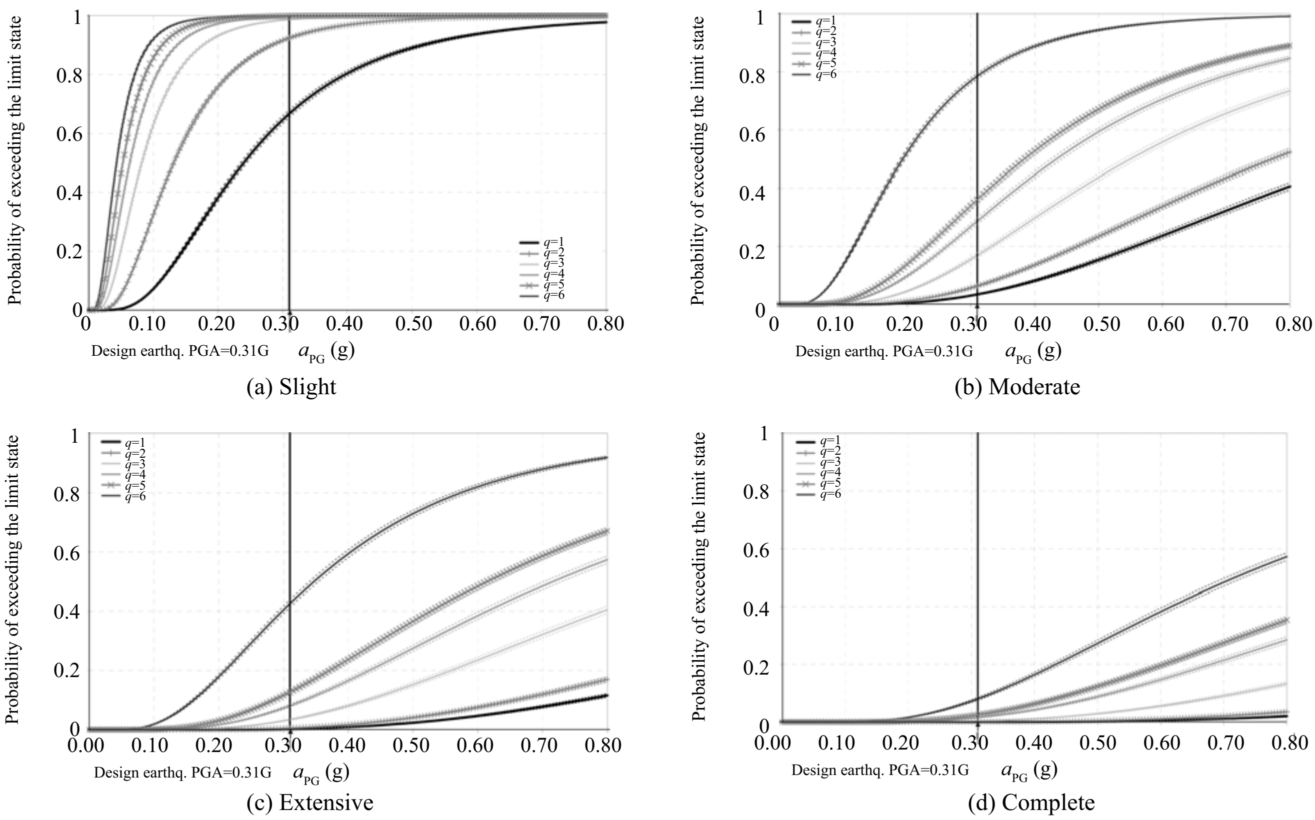

(a) Slight (b) Moderate

(c) Extensive (d) Complete

Fig. 6 Test example 2 - Fragility curves for the four limit states and their confidence intervales

state for the $D_{q=1}$ design is one order of magnitude less than the corresponding probability of the other two designs (3.5% versus 17.0% and 78%, respectively). For the Complete damage state, the probability of exceedance for the $D_{q=1}$ design is two and three orders of magnitude less than the corresponding probability of $D_{q=3}$ and $D_{q=6}$ designs, respectively. Comparing the values of Table 6 with those of Table 3, note that the behavior of the $D_{q=1}$ design is similar to the fully infilled design of the previous test example in terms of probabilities of exceedance for the design earthquake for all four limit states.

In order to define the 95% confidence intervals for all fragility curves, as in the previous test example, two sources of randomness were taken into account: (i) those affecting the structural capacity; and (ii) those affecting the seismic demand. Details on the two sources of randomness are given in Table 7. The confidence intervals for the four sets of fragility curves are also depicted in Figs. 6(a) to 6(d), while the 95% confidence intervals of the probability of exceedance of the four limit states for the design earthquake are given in Table 6.

Table 6 Test example 2 - Limit-state probability of exceedance %

Limit state		q=1	q=2	q=3	q=4	q=5	q=6
Slight	Mean	66.71	92.44	98.69	99.60	99.85	99.95
	+	67.94	92.91	98.79	99.63	99.86	99.96
	-	65.50	91.96	98.57	99.56	99.83	99.95
Moderate	Mean	3.44	6.38	16.92	28.68	36.09	78.49
	+	3.70	6.82	17.75	29.81	37.33	79.45
	-	3.20	5.98	16.13	27.59	34.88	77.53
Extensive	Mean	0.27	0.56	3.41	8.12	12.69	42.54
	+	0.30	0.61	3.66	8.61	13.40	43.87
	-	0.25	0.51	3.17	7.66	12.01	41.25
Complete	Mean	0.01	0.03	0.35	1.57	2.52	8.05
	+	0.02	0.04	0.39	1.71	2.72	8.56
	-	0.01	0.03	0.32	1.45	2.33	7.58

Table 7 Test example 2 - Characteristics of the random variables

Parameter	Distribution	Mean value	COV	Correlation
Confined concrete				
f_c (MPa)	Normal	16.0	0.15	0.3
$\varepsilon_{c,y}$	Normal	0.002	0.15	0.3
$\varepsilon_{c,u}$	Normal	0.0035	0.15	0.3
Unconfined concrete				
f_c (MPa)	Normal	12.8	0.15	0.3
$\varepsilon_{c,y}$	Normal	0.002	0.15	0.3
$\varepsilon_{c,u}$	Normal	0.0035	0.15	0.3
E_c (GPa)	Normal	28.0	0.15	0.3
Steel				
f_y (MPa)	Normal	500.0	0.05	0.5
E_s (GPa)	Normal	200.0	0.05	0.5
Seismic action				
Seismic load	Lognormal	$\hat{x}$ (Eq. (6))	δ (Eq. (7))	0.0

7 Conclusions

The main purpose this study was to examine the effectiveness of fragility analysis in order to assess the seismic performance of multi-story RC buildings designed based on modern codes. For this reason, a parametric study was performed considering two groups of buildings. In the first example, weak ground story and short column construction features were examined, while in the second example, six different designs were obtained that implemented different values of the behavior factor. Fragility analysis were shown to be an efficient tool for assessing the behavior of a structural system. Three significant findings were observed:

(i) The probability of exceedance of the slight damage state for the design earthquake is of the same order for all three designs. On the other hand, it was found that the probability of exceedance for the fully infilled design is one and three orders of magnitude less than that of the other two designs for the moderate and complete damage states, respectively.

(ii) Similar observations were noted for the structure designed for q=1 compared to those designed for larger values of the behavior factor. More specifically, the probability of exceedance of the moderate damage state for the $D_{q=1}$ design is one order of magnitude less than that of the other $D_{q=3}$ and $D_{q=6}$ designs, while for the complete damage state, the probability of exceedance for the $D_{q=1}$ design is two and three orders of magnitude less than the corresponding probability for $D_{q=3}$ and $D_{q=6}$ designs, respectively.

(iii) Furthermore, an important observation of this study can be obtained by comparing the results of the two test examples studied. Through this comparison, it was found that the behavior, in terms of limit-state probability of exceedance for the design earthquake, of the bare design obtained for q=1 is similar to that of the fully infilled design obtained for q=3.5.

References

Aslani H and Miranda E (2005), "Probability-based Seismic Response Analysis," *Engineering Structures*, **27**(8): 1151-1163.

Chao HH, Yungting AT and Ruo YH (2006), "Nonlinear Pushover Analysis of Infilled Concrete Frames," *Earthquake Engineering and Engineering Vibration*, **5**(2): 245-255.

Chintanapakdee C and Chopra AK (2003), "Evaluation of Modal Pushover Analysis Using Generic Frames," *Earthquake Engineering and Structural Dynamics*, **32**(3): 417-442.

Dolšěk M and Fajfar P (2001), "Soft Storey Effects in Uniformly Infilled Reinforced Concrete Frames," *Journal of Earthquake Engineering*, **5**(1): 1-12.

EAK 2000, National Seismic Code of Hellas, 2000.

EKOS 2000, National Code for Concrete Building Structures of Hellas, 2000.

Ellingwood BR (2001), "Earthquake Risk Assessment of Building Structures," *Reliability Engineering and System Safety*, **74**(3): 251-262.

EN 1992-1-1:2002. *Eurocode 2*: Design of Concrete Structures. Part 1: General Rules and Rules for Buildings, Commission of the European Communities, European Committee for Standardization, November 2002.

EN 1998-1:2003. *Eurocode 8*: Design of Structures for Earthquake Resistance. Part 1: General Rules, Seismic Actions and rules for Buildings. Commission of the European Communities, European Committee for Standardization, October 2003.

Fajfar P (1998), "Towards Nonlinear Methods for the Future Seismic Codes," in Booth, ed., *Seismic Design Practice into the Next Century*, Balkema.

FEMA-National Institute of Building Sciences. HAZUS-MH MR1, Multi-hazard Loss Estimation Methodology Earthquake Model, Washington, DC, 2003.

Ghobarah A (2004), "On Drift Limits Associated with Different Damage Levels," *International Workshop on Performance-based Seismic Design*, June 28-July 1.

Ghobarah A, Saatcioglu M and Nistor I (2006), "The Impact of the 26 December 2004 Earthquake and Tsunami on Structures and Infrastructure," *Engineering Structures*, **28**(2): 312-326.

Guevara LT and García LE (2005), "The Captive- and Short-column Effects," *Earthquake Spectra*, **21**(1): 141-160.

Jeong SH and Elnashai AS (2007), "Probabilistic Fragility Analysis Parameterized by Fundamental Response Quantities," *Engineering Structures*, **29**(6): 1238-1251.

Kappos AJ, Panagopoulos G, Panagiotopoulos C and Penelis G (2006), "A hybrid Method for the Vulnerability Assessment of R/C and URM buildings," *Bulletin of Earthquake Engineering*, **4**(4): 391-413.

Kennedy, RP, Cornell, CA, Campbell RD, Kaplan S and Perla HF (1980), "Probabilistic Seismic Safety Study of an Existing Nuclear Power Plant," *Nuclear Engineering and Design*, **59**(2): 315-338.

Kircher CA, Nassar AA, Kustu O and Holmes WT (1997), "Development of Building Damage Functions for Earthquake Loss Estimation," *Earthquake Spectra*, **13**(4): 663-682.

Lagaros ND (2007), "Life-cycle Cost Analysis of Design Practices for RC Framed Structures," *Bulletin of Earthquake Engineering*, **5**(3):425-442.

Lagaros ND, Fotis AD and Krikos SA (2006), "Assessment of Seismic Design Procedures Based on the Total Cost," *Earthquake Engineering and Structural Dynamics*, **35**(11): 1381-1401.

Lee HS and Woo SW (2002), "Effect of Masonry Infills on Seismic Performance of a 3-storeystory R/C Frame with Non-seismic Detailing," *Earthquake Engineering and Structural Dynamics*, **31**(2): 353-378.

Li ZX (2005), "Theory and Technology of Split Reinforced Concrete Columns," *Engineering Mechanics*, **22**: 127-141.

Mazzolani FM and Piluso V (1996), *The Theory and Design of Seismic Resistant Steel Frames*, E & FN Spon.

McKenna F and Fenves GL (2001), *The OpenSees Command Language Manual - Version 1.2*, Pacific Earthquake Engineering Research Centre, University of California, Berkeley.

Mitchell D, DeVall RH, Kobayashi K, Tinawi R and Tso WK (1996), "Damage to Concrete Structures due to the January 17, 1995, Hyogo-ken Nanbu (Kobe) Earthquake," *Canadian Journal of Civil Engineering*, **23**(3): 757-770.

Negro P and Verzeletti G (1996), "Effect of Infills on the Global Behaviourbehavior of R/C Frames: Energy Considerations from Pseudodynamic Tests," *Earthquake Engineering and Structural Dynamics*, **25**(8): 753-773.

Pagni CA and Lowes LN (2006), "Fragility Functions for Older Reinforced Concrete Beam-column Joints," *Earthquake Spectra*, **22**(1):215-238.

Papazachos BC, Papaioannou ChA and Theodulidis NP (1993), "Regionalization of Seismic Hazard in Greece Based on Seismic Sources," *Natural Hazards*, **8**(1): 1-18.

Perera R, Gomez S and Alarcon E (2004), "Experimental and Analytical Study of Masonry Infill Reinforced Concrete Frames Retrofitted with Steel Braces," *Journal of Structural Engineering*, **130**(12): 2032-2039.

Porter K, Kennedy R and Bachman R (2007), "Creating Fragility Functions for Performance-based Earthquake Engineering," *Earthquake Spectra*, **23**(2):471-489.

Shinozuka M, Feng MQ, Lee J and Naganuma T (2000), "Statistical Analysis of Fragility Curves," *Journal of Engineering Mechanics*, **126**(12): 1224-1231.

Shinozuka M, Murachi Y, Dong X, Zhou Y and Orlikowski MJ (2003), "Effect of Seismic Retrofit of Bridges on Transportation Networks," *Earthquake Engineering and Engineering Vibration*, **2**(2): 169-179.

Somerville P and Collins N (2002), "Ground Motion Time Histories for the Humboldt Bay Bridge," Pasadena, CA, URS Corporation.

Wen YK and Ellingwood BR (2005), "The Role of Fragility Assessment in Consequence-based Engineering," *Earthquake Spectra*, **21**(3): 861-877.